



HAL
open science

Modeling Natural Tritium in Precipitation and its Dependence on Decadal Solar Activity Variations Using the Atmospheric General Circulation Model MIROC5-Iso

Alexandre Cauquoin, Élise Fourré, Amaelle Landais, Atsushi Okazaki, Kei
Yoshimura

► **To cite this version:**

Alexandre Cauquoin, Élise Fourré, Amaelle Landais, Atsushi Okazaki, Kei Yoshimura. Modeling Natural Tritium in Precipitation and its Dependence on Decadal Solar Activity Variations Using the Atmospheric General Circulation Model MIROC5-Iso. *Journal of Geophysical Research: Atmospheres*, 2024, 129 (5), 10.1029/2023jd039745 . hal-04488257

HAL Id: hal-04488257

<https://hal.science/hal-04488257>

Submitted on 4 Mar 2024

HAL is a multi-disciplinary open access archive for the deposit and dissemination of scientific research documents, whether they are published or not. The documents may come from teaching and research institutions in France or abroad, or from public or private research centers.

L'archive ouverte pluridisciplinaire **HAL**, est destinée au dépôt et à la diffusion de documents scientifiques de niveau recherche, publiés ou non, émanant des établissements d'enseignement et de recherche français ou étrangers, des laboratoires publics ou privés.

JGR Atmospheres

RESEARCH ARTICLE

10.1029/2023JD039745

Key Points:

- For the first time, natural tritium (HTO) is modeled in an atmospheric model by considering solar modulation over the period 1979–2018
- MIROC5-iso correctly captures the observed spatial distribution of tritium in precipitation and its temporal variations
- Internal climate modes can enhance or hide changes in tritium in precipitation owing to the decadal tritium production variations

Supporting Information:

Supporting Information may be found in the online version of this article.

Correspondence to:

A. Cauquoin,
cauquoin@iis.u-tokyo.ac.jp

Citation:

Cauquoin, A., Fourré, É., Landais, A., Okazaki, A., & Yoshimura, K. (2024). Modeling natural tritium in precipitation and its dependence on decadal solar activity variations using the atmospheric general circulation model MIROC5-iso. *Journal of Geophysical Research: Atmospheres*, 129, e2023JD039745. <https://doi.org/10.1029/2023JD039745>

Received 31 JULY 2023

Accepted 16 FEB 2024

Author Contributions:

Conceptualization: A. Cauquoin

Data curation: A. Cauquoin, É. Fourré, A. Landais, A. Okazaki

Formal analysis: A. Cauquoin

Funding acquisition: A. Cauquoin, K. Yoshimura

Investigation: A. Cauquoin, É. Fourré, A. Landais

Methodology: A. Cauquoin

Project administration: A. Cauquoin

Resources: K. Yoshimura

Software: A. Cauquoin, A. Okazaki, K. Yoshimura

Supervision: A. Cauquoin, K. Yoshimura

Validation: A. Cauquoin

© 2024. The Authors.

This is an open access article under the terms of the [Creative Commons Attribution License](https://creativecommons.org/licenses/by/4.0/), which permits use, distribution and reproduction in any medium, provided the original work is properly cited.

Attribution License, which permits use, distribution and reproduction in any medium, provided the original work is properly cited.

Modeling Natural Tritium in Precipitation and its Dependence on Decadal Solar Activity Variations Using the Atmospheric General Circulation Model MIROC5-Iso

A. Cauquoin¹ , É. Fourré² , A. Landais², A. Okazaki^{3,4} , and K. Yoshimura¹ 

¹Institute of Industrial Science (IIS), The University of Tokyo, Kashiwa, Japan, ²Laboratoire des Sciences du Climat et de l'Environnement, LSCE, CEA, CNRS, UVSQ, IPSL, Université Paris-Saclay, Paris, France, ³Department of Global Environment and Disaster Prevention Sciences, Hirosaki University, Hirosaki, Japan, ⁴Institute for Advanced Academic Research / Center for Environmental Remote Sensing, Chiba University, Chiba, Japan

Abstract Modeling tritium content in water presents a meaningful way to evaluate the representation of the water cycle in climate models as it traces fluxes within and between the reservoirs involved in the water cycle (stratosphere, troposphere, and ocean). In this study, we present the implementation of natural tritium in water in the atmospheric general circulation model (AGCM) MIROC5-iso and its simulation for the period 1979–2018. Owing to recently published tritium production calculations, we were able to investigate, for the first time, the influence of natural tritium production related to the 11-yr solar cycle on tritium in precipitation. MIROC5-iso correctly simulates continental, latitudinal, and altitude effects on tritium in precipitation. The seasonal tritium content peaks, linked to stratosphere-troposphere exchanges, are accurately simulated in terms of timing, even though MIROC5-iso underestimates the amplitude of the changes. Decadal tritium concentration variations in precipitation owing to the 11-yr solar cycle are well simulated in MIROC5-iso, in agreement with the observations at Vostok in Antarctica for example. Finally, our simulations revealed that the internal climate variability plays an important role in tritium in polar precipitation. Owing to its influence on the south polar vortex, the Southern Annular Mode enhances the effect of the production component on tritium in East Antarctic precipitation. In Greenland, we found an east-west contrast in the detection of the 11-yr solar cycle in tritium in precipitation owing to the influence of the North Atlantic Oscillation on humidity conditions.

Plain Language Summary Models used to simulate the future of our climate are still struggling to represent the water cycle adequately. To address this challenge, we have added the capability to simulate tritium in water into the atmospheric model MIROC5-iso. Tritium is a naturally occurring radioactive isotope produced by interactions of cosmic rays in the atmosphere. Because it decays away with a half-life of 12.32 years, it is a very powerful tracer of water exchanges within and between water cycle reservoirs, such as the stratosphere, the troposphere, and the ocean. We were also able to investigate the influence of the 11-year solar cycle on tritium in precipitation, as well as the impact of natural atmospheric circulation variations on an interannual time scale. MIROC5-iso can simulate decadal variations in tritium in precipitation related to solar cycles. The presence or absence of this cycle in our modeled tritium for polar regions is influenced by interannual variations in the atmospheric circulation, especially related to precipitation amount variations. Conclusively, we show that tritium is reliable complementary tracer for better constraining the water cycle representation in climate models.

1. Introduction

A primary challenge for the climate research community is to improve the hydrological cycle representation in general circulation models (GCMs). These models are used to study the Earth's climate system and project future changes. Water isotopologues simulation is a useful way to evaluate the performance of these models. Stable water isotopologues, such as H₂¹⁶O, H₂¹⁸O, and H²H¹⁶O, are widely used in atmospheric GCMs (AGCMs) as tracers of past and present-day climate processes recorded in the hydrological cycle (Cauquoin & Werner, 2021; Joussaume et al., 1984; Jouzel et al., 1987; Lee et al., 2007; Noone & Simmonds, 2002; Nusbaumer et al., 2017; Okazaki & Yoshimura, 2019; Risi et al., 2010; Werner et al., 2011; Yoshimura et al., 2008).

Once produced in the atmosphere, tritium (*T*) atoms enter the hydrological cycle in the form of tritiated water (HTO) for a vast majority (Gat et al., 2001), presenting another useful water isotopologue with different characteristics. As stable water isotopologues, HTO is thus influenced by the same fractionation effects during water

Visualization: A. Cauquoin

Writing – original draft: A. Cauquoin

Writing – review & editing:

A. Cauquoin, É. Fourné, A. Landais,

A. Okazaki, K. Yoshimura

phase changes (Cauquoin et al., 2015), and is transported in the same way through the water cycle. Therefore, they are both influenced by the isotopic content of the source of precipitation through horizontal (e.g., from the ocean) and vertical (e.g., downward motion) transport, which are dynamical atmospheric processes. However, in the case of tritium, the fractionation effects are attenuated or even masked by its other characteristics such as cosmogenic production and radioactive decay.

According to Poluianov et al. (2020), natural tritium is mainly produced by the interaction of galactic cosmic rays (GCRs, which are high-energy charged particles and their secondary products) with nitrogen atoms of the upper atmosphere at an average rate of 0.345 atoms/(s m²), close to previous estimates (Craig & Lal, 1961; Masarik & Beer, 2009). Tritium has a radioactive half-life of 12.32 ± 0.02 years (Lucas & Unterweger, 2000). Because of the higher tritium production at the top of the atmosphere and dryer air at higher altitudes, the tritium level in surface water vapor and in precipitation is only a few tritium units (TU; 1 TU corresponds to a T/H ratio of 10⁻¹⁸) (IAEA, 2023; Terzer-Wassmuth et al., 2022a) whereas it reaches more than 10⁵ TU in the stratosphere (Cauquoin et al., 2015; Ehhalt et al., 2002; Fourné et al., 2006). Because of these characteristics, which cause tritium in water vapor to vary by orders of magnitude in the different components involved in the water cycle (e.g., troposphere, stratosphere, and ocean), HTO represents an extremely valuable marker to evaluate fluxes between these reservoirs. The large stratospheric reservoir makes HTO a very good tracer of stratospheric air intrusions in the troposphere (Cauquoin et al., 2015; Fourné et al., 2006; Jouzel et al., 1979, 1982).

Large amounts of anthropogenic tritium from nuclear tests were injected into the atmosphere mainly during the 1950–1960s. These injections led to a substantial increase in the global inventory of tritium, by approximately two orders of magnitude (520–550 kg (Michel, 1976; UNSCEAR, 2000) compared with 3.6 kg natural tritium (Fourné et al., 2006)). These tests have caused a “tritium peak” measured in the precipitation of 1963–1964 that was several orders of magnitude higher than the natural level (IAEA, 2023). Since the Nuclear Test Ban Treaty in 1963, the tritium level in precipitation has continuously decreased owing to radioactive decay and mixing with tritium-free ocean water. Consequently, tritium content in precipitation has reached a level close to that of the pre-bomb period (Terzer-Wassmuth et al., 2022a), enabling the use of the natural tritium variability to study water vapor transport linked to climate processes, stratospheric moisture inputs in Antarctica, or past changes in solar activity (Cauquoin et al., 2015; Fourné et al., 2018; Juhlke et al., 2020; Palsu et al., 2018).

Since the pioneering work of Koster et al. (1989), the natural and anthropogenic components of HTO have been implemented in the isotope-enabled AGCM LMDZ-iso (Cauquoin et al., 2015, 2016). It was the first time that this tracer was implemented in a state-of-the-art AGCM. Before reaching the Earth's atmosphere, GCRs are modulated by the magnetic shields of the Sun (heliomagnetic field or solar activity) and the Earth (geomagnetic field). In other words, the higher the solar activity or the geomagnetic shielding, the more GCR particles are deflected, and less tritium is produced. Cauquoin et al. (2015) used constant tritium production rates over time from Masarik and Beer (2009) for the long-term average value of the solar activity and the present-day value of the geomagnetic field strength. Poluianov et al. (2020) provided a new model of cosmogenic (i.e., natural) tritium production in the atmosphere, called CRAC:3H. Compared with Masarik and Beer (2009), CRAC:3H can compute tritium production at any location and time, for any given energy spectrum of the primary incident cosmic ray particles, explicitly treating particles heavier than protons. Therefore, the effects of past variations in solar activity and geomagnetic field on tritium in precipitation, which have not been considered in previous studies using modeled tritium outputs (Cauquoin et al., 2015, 2016; Fourné et al., 2018), can now be investigated. Finally, several reanalysis datasets have been produced in recent years, such as the Japanese 55-year Reanalysis, known as JRA-55 (Harada et al., 2016; Kobayashi et al., 2015). These reanalyses boast improved quality owing to advances in operational data assimilation and the incorporation of extensive observational data over an extended period. Such reanalysis improvements are expected to improve the weather conditions modeling in nudged AGCM simulations. As tritium in precipitation is also influenced by climatic effects on the water cycle (Fourné et al., 2018), it provides an opportunity to investigate in more details how internal climate variability and natural tritium production control the levels of tritium in precipitation.

In this study, we present, for the first time, the HTO modeling in an isotope-enabled AGCM (MIROC5-iso, see Section 2.1) by considering cosmogenic tritium production changes due to solar activity variations for the period of 1979–2018. This represents a clear step forward compared with previous tritium modeling studies (Cauquoin et al., 2015, 2016; Fourné et al., 2018). As we focus here on the natural variations in HTO related to cosmogenic production changes, moisture transport between the stratosphere and the troposphere, and

interannual climate variability, no bomb-tritium inputs were added in this modeling exercise. The remainder of this paper is organized as follows. In Section 2, we briefly describe the model used, the HTO implementation, and datasets used for model evaluation. In Section 3, we evaluate the spatial distribution and temporal variability of the modeled HTO in precipitation and water vapor. In Section 4, we investigate the factors controlling tritium content variations in precipitation, particularly in polar regions where past changes in tritium can be measured in snow pits. Finally, we conclude the paper with a summary of our findings and future perspectives in Section 5.

2. Model Simulations and Datasets

2.1. MIROC5-Iso

MIROC5-iso (Okazaki & Yoshimura, 2019) is the atmospheric-land component of the fifth version of Model for Interdisciplinary Research on Climate, Earth System Model (MIROC5) (Watanabe et al., 2010), equipped with stable water isotopes. The model uses the Chikira-Sugiyama cumulus scheme (Chikira & Sugiyama, 2010), which is an entraining plume model, for convective parameterization, a semi-Lagrangian scheme for the advection of tracers including the water in its vapor and condensed states (Lin & Rood, 1996), and an orographic gravity wave drag parameterization from McFarlane (1987). A large-scale condensation scheme from Watanabe et al. (2009) and a bulk microphysical scheme (Wilson & Ballard, 1999) are used for the representation of clouds and cloud-radiative feedback. On the surface, the land component of MIROC5, called Minimal Advanced Treatments of Surface Interaction and RunOff (MATSIRO), is used (Nitta et al., 2014; Takata et al., 2003). The implementation of stable water isotopes in this component to model, for example, soil surface evaporation, vegetation transpiration, and evaporation from the canopy-intercepted reservoir, has been previously described by Yoshimura et al. (2006).

HTO differs from other water isotopologues in terms of cosmogenic production and radioactivity. In contrast, similar to what was done for LMDZ-iso (Cauquoin et al., 2015), the physical and dynamical descriptions of the HTO molecule are the same as those for the other water isotopologues in MIROC5-iso. Similar to the heavier isotopologues H_2^{18}O and $\text{H}_2\text{H}^{16}\text{O}$, HTO is subject to fractionation processes at each phase change due to differences in mass and symmetry. Most fractionations in phase transitions are assumed to occur at thermodynamic equilibrium. The temperature-dependent coefficients for the equilibrium fractionation (α_{eq}) between vapor and liquid water or ice for HTO were obtained from Koster et al. (1989). At a temperature of 10°C, the coefficient for liquid/vapor fractionation is 1.2373 for HTO/ H_2^{16}O fractionation, which is higher than the value for $\text{H}_2^{18}\text{O}/\text{H}_2^{16}\text{O}$ fractionation ($\alpha_{\text{eq}} = 1.0107$). Similar to stable isotopologues, kinetic isotopic fractionation (α_{kin} coefficient) of HTO occurs during surface evaporation from open water, following Merlivat and Jouzel (1979). Evaporation and isotopic exchange from falling droplets into unsaturated air were implemented according to the methods of Stewart (1975) and Yoshimura et al. (2008). Air supersaturation, with respect to ice when vapor condenses in the frozen form, is assumed to occur at temperatures below $T = -20^\circ\text{C}$. The effective fractionation (α_{eff}) is expressed as a function of α_{eq} between vapor and ice, molecular diffusivities, and supersaturation over ice $S = 1 - 0.003 T$ based on Jouzel et al. (1987). The effective fractionation, α_{eff} , was obtained from Jouzel and Merlivat (1984) as follows:

$$\alpha_{\text{eff}} = \alpha_{\text{eq}} \left[\frac{S}{1 + \alpha_{\text{eq}}(S - 1)D/D'} \right] \quad (1)$$

where D and D' are the molecular diffusivities in air of H_2^{16}O and the heavier isotopologue, respectively. The diffusivity of HTO was derived from Merlivat (1978) as 0.968 times that of H_2^{16}O .

2.2. Natural Tritium Production Implementation

As GCRs are modulated by the magnetic shields of the Sun and Earth before reaching the atmosphere, natural tritium production is inversely related to solar activity and the geomagnetic field. Cosmogenic tritium production has a strong latitudinal dependence caused by the geomagnetic modulation with a stronger shielding effect at the geomagnetic equator (Lal & Peters, 1967; Masarik & Beer, 2009; Poluianov et al., 2020). The dependency of tritium production on altitude is expressed by the trade-off between the energy of the secondary particles

produced by the GCR (decreasing with atmospheric pressure owing to spallation reactions and geomagnetic rigidity) and their numbers (increasing with atmospheric pressure).

In this study, we used the production rates of Poluianov et al. (2020) and Masarik and Beer (2009), hereafter referred to as CRAC:3H and MB2009, respectively. For simulations with constant tritium production rates over time (i.e., with no change in solar activity), we used the long-term average values for the modern period recommended by the authors of each of these publications. For MB2009, a solar modulation parameter $\phi = 550$ MV (local interstellar spectrum from Castagnoli and Lal (1980)) and a relative geomagnetic field intensity $B = 1$ were set, as per Cauquoin et al. (2015). For CRAC:3H, the production rate values for $\phi = 650$ MV (local interstellar spectrum from Vos and Potgieter (2015)) and geomagnetic cutoff rigidities from the International Geomagnetic Reference Field (IGRF (Thébault et al., 2015),) for the epoch 2015 were used. Finally, because the CRAC:3H model can compute cosmogenic tritium production at any location and time, considering changes in the modulation of incident GCR particles, we also used monthly mean production rates from January 1979 to December 2018, with varying solar modulation potentials from Usoskin et al. (2017) and geomagnetic cutoff rigidity from the IGRF-13 model (Alken et al., 2021). Variations in the geomagnetic cutoff rigidity occur over a considerable period of time compared to variations in the solar modulation potential. Similar to Cauquoin et al. (2015), we assume that one tritium atom produced corresponds to one HTO molecule.

2.3. Simulations

To evaluate the effects of the transition from MB2009 to CRAC:3H production rates and the impact of solar activity changes over the period of 1979–2018 on the modeled HTO by MIROC5-iso, we performed three simulations: (a) MB2009_3H_cte: with constant long-term average production rate values over time from MB2009; (b) CRAC_3H_cte: with constant long-term average production rate values over time from CRAC:3H model; (c) CRAC_3H_solar: with monthly mean tritium production rate variations from CRAC:3H model due to modulation of GCR by heliomagnetic and geomagnetic fields over time.

All MIROC5-iso simulations were performed at T42L40 spatial resolution (approximately 2.8° horizontal resolution and 40 vertical levels up to 3 hPa). MIROC5-iso simulations were nudged to the U and V components of winds from JRA-55 reanalyses (Harada et al., 2016; Kobayashi et al., 2015) every six hours for the period of 1979–2018. Compared with JRA-55, the 20CR reanalyses (Compo et al., 2011) used by Cauquoin et al. (2015, 2016) with LMDZ-iso were created by assimilating a limited set of observations, that is, only surface pressure. JRA-55 uses an advanced data assimilation scheme, increased model resolution (approximately 40 km horizontal resolution and 60 vertical levels), a new variational bias correction for satellite data, and several additional observational data sources (Kobayashi et al., 2015). A spin-up was performed at the start of all simulations by modeling the weather conditions of 1979 for 30 consecutive model years. Orbital parameters and greenhouse gases concentrations were set to the values of the corresponding model years following the Coupled Model Intercomparison Project Phase 6 protocol (CMIP6 (Eyring et al., 2016)). The six-hourly mean sea surface temperature (SST) and sea ice area fraction fields from the JRA-55 reanalyses were applied as sea surface boundary conditions. For the $\delta^{18}\text{O}$ ($\text{H}_2^{18}\text{O}/\text{H}_2^{16}\text{O}$ ratio expressed relative to V-SMOW standard) sea surface boundary conditions, we assumed a constant value over time of 0 ‰. For tritium sea surface boundary concentrations, we assumed constant values over time using the map reconstructed by Cauquoin et al. (2016) from available tritium data for the year 2004, which is the most recent year available in this reconstruction, when the global tritium content nearly reached natural pre-bomb level (see Figure S1 in Supporting Information S1). These values are probably slightly higher than the 2008–2018 averaged ones, especially in the Atlantic Ocean, potentially contributing to a positive bias in tritium levels in coastal sites. However, we do not expect large biases for inland sites, as shown by Cauquoin et al. (2016) who used spatially constant sea surface concentration of 0.2 TU for one of their sensitivity simulations.

2.4. Observational Data

To analyze the results of our simulations, tritium data that are as unpolluted as possible by the anthropogenic signal from nuclear bomb testing were used. To evaluate the mean spatial distribution of natural tritium in precipitation modeled by MIROC5-iso, we used the pre-bomb tritium data compiled by Cauquoin et al. (2015). These data were obtained from rainwater, freshwater reservoirs, and ice cores. We excluded the extrapolated data from the Global Network of Isotopes in Precipitation series (GNIP; database available through the International

Atomic Energy Agency (IAEA, 2023)). Because only a few data points were available, we also used the dataset of contemporary tritium in precipitation data from Terzer-Wassmuth et al. (2022a). They compiled these “post-bomb” data from the GNIP dataset and other published data (see their Supplementary Material in Supporting Information S1) for the period of 2008–2018, considering an impact as low as possible of the anthropogenic signal on tritium content in precipitation and data availability. To evaluate the modeled seasonal variations in tritium, we selected five GNIP stations (IAEA, 2023) with well-resolved monthly mean tritium observations in precipitation, also for the period 2008–2018: Vienna (inland Europe), Valentia (coastal Europe), Ottawa (North America), Kaitoke (South Pacific), and Halley Bay (Antarctica). Finally, we used snow pits tritium content measurements from Vostok, East Antarctica (Fourré et al., 2018) to investigate the impact of solar activity and the internal modes of atmospheric circulation on tritium in precipitation from Central Antarctica.

3. Evaluation of MIROC5-Iso Modeled Tritium Distribution

3.1. Global Spatial Distribution of Tritium in Water Vapor and Precipitation

3.1.1. Vertical Profile of Tritium in Water Vapor

Here, we evaluate the mean spatial distribution of tritium content in water vapor for the same period as contemporary tritium data (Terzer-Wassmuth et al., 2022a) that is, 2008–2018. The tritium level in water vapor near the surface is only a few TU, whereas it reaches more than 10^6 TU in the highest vertical layers of MIROC5-iso (Figure 1a, CRAC_3H_cte simulation). The mean tritium content at pressure levels +200 hPa level (i.e., in the stratosphere) varies between 5.28×10^5 and 5.73×10^5 TU in our different simulations, slightly higher than that in the modeling study of Cauquoin et al. (2015) and similar to observations (Ehhalt et al., 2002; Fourré et al., 2006). Similar to Cauquoin et al. (2015), latitudinal variations in tritium content in water vapor are modeled by MIROC5-iso, with higher and lower values at the poles and the equatorial region, respectively, owing to the strong latitudinal dependency of cosmogenic tritium production (Masarik & Beer, 2009; Poluianov et al., 2020). We find similar spatial patterns and orders of magnitude in the tritium levels for the three simulations. The use of CRAC:3H production rates instead of the calculations from Masarik and Beer (2009) for natural tritium production input increases the tropospheric tritium concentration in the middle to high latitudes by a factor of 1.45 (Figure 1b). In contrast, it slightly decreases the tritium contents in the equatorial tropopause and at altitude above the 100 hPa level. These differences could be attributable particles heavier than protons for tritium production in CRAC:3H, uncertainties in the cross-sections of nuclear reactions, or details in the cosmic-ray-induced atmospheric cascade (Poluianov et al., 2020). Moreover, the long-term present-day conditions for tritium production are not exactly the same in the CRAC:3H and MB2009 calculations (Section 2.2).

3.1.2. Spatial Distribution of Tritium in Precipitation

The mean spatial distribution of the modeled tritium content of precipitation from the three simulations for the period 2008–2018, with pre-bomb and contemporary data, is evaluated on Figure 2. A clear ocean-land contrast is visible in both the observations and model results, with lower and higher TU values in the ocean and land, respectively (Figure 2a–2g). This continental effect is due to tritium production incorporated into precipitation and continental water mass evaporation, whereas tritium in marine re-evaporation remains low because of the strong influence of tritium-free ocean water. An increasing trend from the Atlantic Ocean (1–2 TU) to Eurasia (4.5–6 TU) is modeled by MIROC5-iso (Figures 2b–2h), lower than the observed gradient (>10 TU in Eurasia). The continental gradient of MIROC5-iso is also lower than that of the pre-bomb data but to a lesser extent (Figure 2c–2i). This could indicate the presence of residual bomb-tritium in contemporary data. Moreover, a bias in the modeled land surface evapotranspiration could also partly explain the underestimation of MIROC5-iso regarding the continental effect. Furthermore, Cauquoin et al. (2015) demonstrated that fractionation during water phase changes amplifies the tritium signal in the upper troposphere (due to fractionation effects during the condensation of vapor into precipitation), thus increasing the continental effect. In our case, this means that an increase in the already quite high fractionation coefficient of Koster et al. (1989) would be necessary, which seems to be an unlikely explanation for our underestimated continental gradient. The latitudinal variation in the tritium content in precipitation, due to the latitudinal dependency of cosmogenic tritium production, is also well reproduced by MIROC5-iso. Latitudinal variation is primarily observed over ocean-covered areas where there are no superimposed continental or altitudinal effects, explaining the large difference in tritium in precipitation

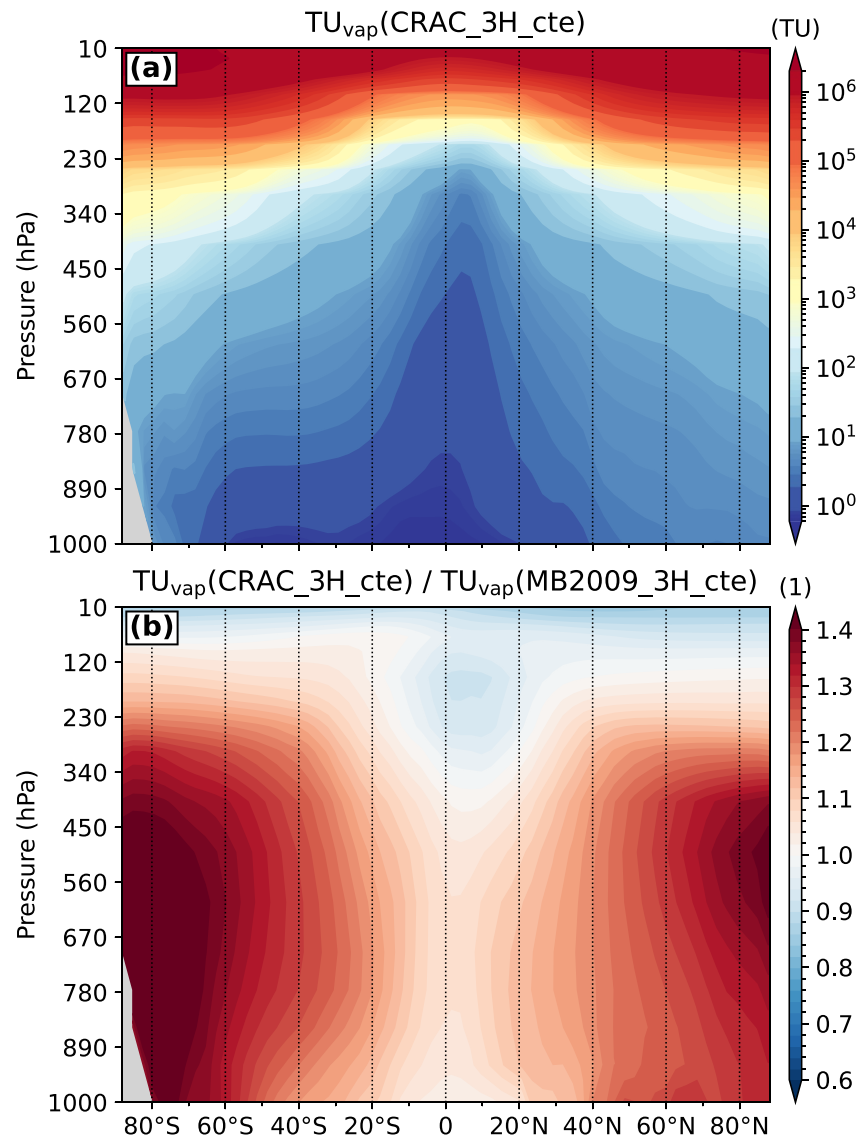


Figure 1. (a) Mean vertical zonal profile of tritium content in water vapor in the CRAC_3H_cte simulation for the period of 2008–2018. (b) Same as (a), but relative to the modeled tritium values in MB2009_3H_cte.

between the northern and southern mid-latitudes. In particular, higher values are found in Antarctica (between 20 and 40 TU according to the MIROC5-iso simulations and up to 60 TU according to the pre-bomb observations), with an increasing continental trend due to seasonal stratospheric air inputs (Roscoe, 2004), higher altitude (higher production), and very dry conditions on the East Antarctic plateau, which attenuate the local dilution of stratospheric moisture inputs in the troposphere. Higher tritium levels are also observed (8–12 TU) and modeled (4–9 TU) in Greenland, but to a lesser extent because there is a greater influence of oceanic water vapor, more humid air, and no polar vortex over this area, such as Antarctica.

Using the CRAC:3H production rate instead of MB2009 increases the model-data slope from 0.37 to 0.51 (Figure 2c and 2f, respectively) and reduces the root mean square error (RMSE) from 5.51 to 4.55 TU. Continental and latitudinal effects are enhanced in the CRAC_3H_solar simulation (Figure 2g and 2h), that is, when using the CRAC:3H production rate and considering changes in solar activity during the period 2008–2018. A better agreement in both contemporary and pre-bomb observations is found using this configuration (model-data slope equal to 0.55 and RMSE = 4.24 TU, Figure 2i).

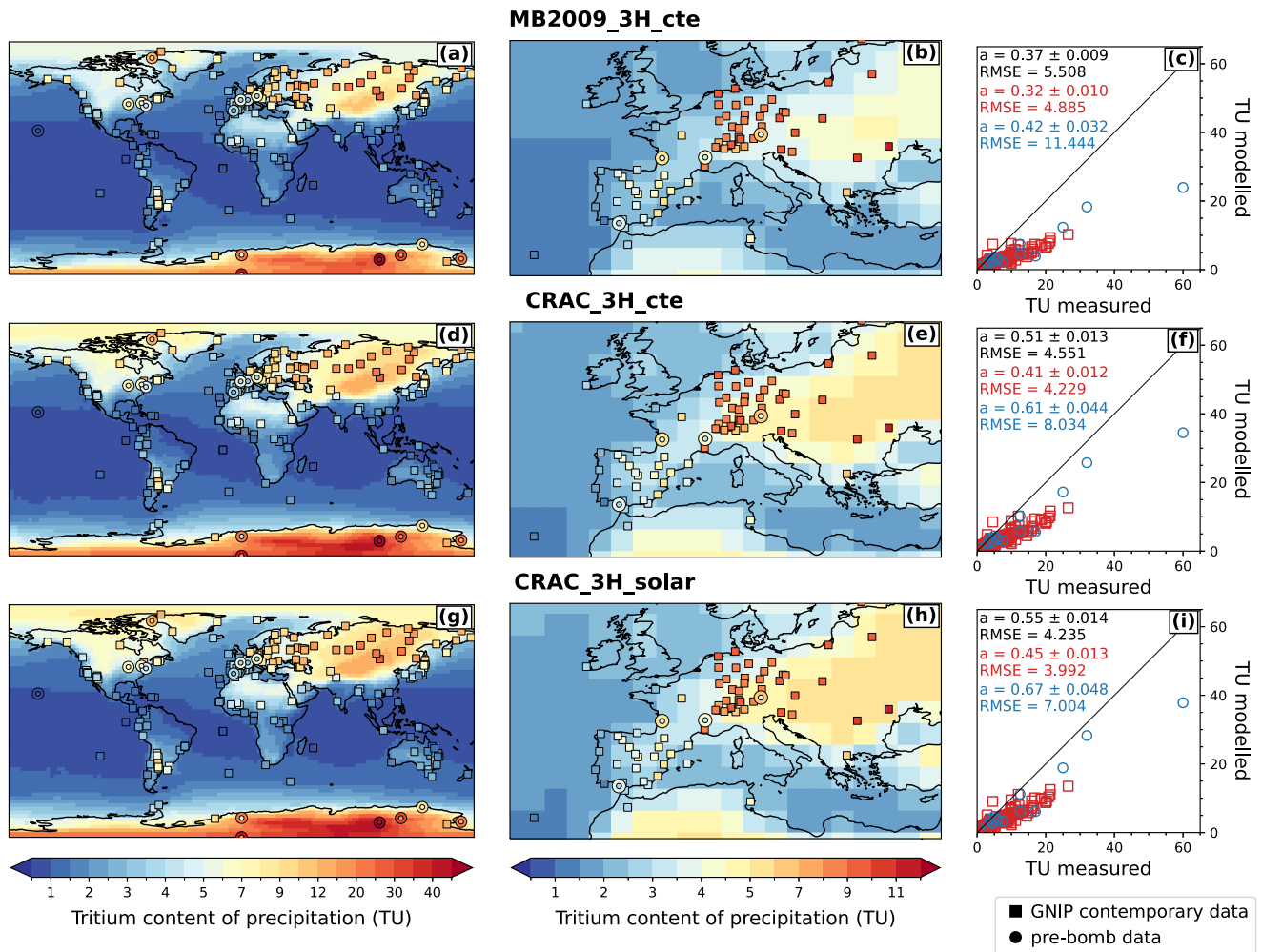


Figure 2. Annual mean tritium content of precipitation for the period of 2008–2018 from our simulations with contemporary (squares) and pre-bomb tritium data (large and small circles for the higher and lower limits, respectively). (a) Global map with MB2009_3H_cte results; (b) MB2009_3H_cte results for the Eurasian region; (c) model-data scatter plot with MB2009_3H_cte results. The gradients of the linear regressions and the root mean square error (RMSE) values are given in the legend for the contemporary data (red), the pre-bomb observations (blue), and collective data (black). The 1:1 black line indicates a perfect model fit. (d), (e) and (f) as (a), (b) and (c) but for the CRAC_3H_cte simulation. (g), (h) and (i) as (a), (b) and (c) but for the CRAC_3H_solar simulation.

3.2. Temporal Variations of Tritium in Precipitation

3.2.1. Seasonal Variability

The tritium in precipitation experiences a seasonal cycle due to the mixing of air masses from the stratosphere to the troposphere, with a maximum in spring (Gat et al., 2001). In the Northern Hemisphere, MIROC5-iso (colored curves in Figure 3) reproduces the timing of the observed seasonal tritium signals well (black curves in Figure 3 for the Vienna, Valentia, and Ottawa stations), with a peak between May and August. This is a clear improvement compared to the modeled results of LMDZ-iso, where unobserved winter peaks were simulated, probably because of the excessive occurrence of rapidly descending air from the stratosphere in wintertime (Cauquoin et al., 2015). MIROC5-iso simulates lower seasonal amplitudes at coastal sites (Valentia) compared to inland sites (Vienna) owing to the influence of marine water vapor, in agreement with observations. In contrast, our model underestimates the amplitude of seasonal changes in the tritium of precipitation. For example, tritium levels between 6 and 12 TU were measured in precipitation of Vienna, whereas variations between 3 and 6 TU only were modeled by MIROC5-iso, only. This finding could be attributable to the presence of remaining “post-bomb” tritium in the data or the under-estimation of modeled continental effect on tritium due to too coarse spatial resolution. The decline by a factor of two in tritium in precipitation from July to November can be explained by

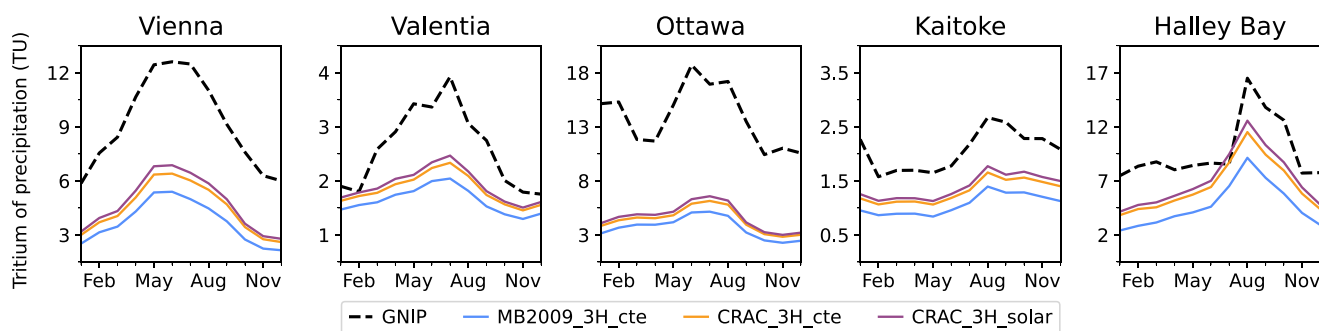


Figure 3. From left to right, mean seasonal variations in tritium content in precipitation for the period of 2008–2018 at Vienna, Valentia, Ottawa, Kaitoke and Halley Bay stations. The dashed black, plain blue, plain orange, and plain purple curves represent the values from GNIP dataset, MB2009_3H_cte, CRAC_3H_cte, and CRAC_3H_solar simulations, respectively.

the stronger incursion of oceanic water (relatively free of tritium) in the European continent, especially from June to September (Figure S2 in Supporting Information S1). In the Southern Hemisphere, the tritium seasonal peak occurring in austral winter and spring (i.e., between July and October) is also well modeled by MIROC5-iso (Kaitoke and Halley Bay stations in Figure 3). The stronger seasonal amplitude observed in both data and simulations at Halley Bay station is due to the presence of a polar vortex above Antarctica during the austral winter, which isolates the continent from marine air masses and enhances the descent of stratospheric moisture rich in tritium. Again, MIROC5-iso simulates too low seasonal amplitudes, probably because of the too strong influence of marine water vapor on these coastal sites. However, our model-data agreement exceeds that of Cauquoin et al. (2015) with the LMDZ-iso model, in which the seasonal amplitude was too strong by a factor of greater than two with the seasonal peak too early by 2 months at Halley Bay. Finally, we find better model-data agreement for all considered sites with the CRAC_3H_solar simulation (orange curves in Figure 3). In contrast, the tritium levels of the MB2009_3H_cte simulation (blue curves in Figure 3) are lower than those of the other two simulations using the CRAC:3H production model, resulting poorer agreement with the observations.

3.2.2. Interannual Variability Due To Solar Activity Changes

Based on CRAC:3H production calculations, we investigated how solar activity changes impact our modeled tritium in precipitation on an interannual time scale (Figure 4). The cosmogenic HTO production from the CRAC_3H_solar simulation (blue curve in Figure 4b) is inversely correlated with the CMIP6 total solar irradiance (TSI), which is used as radiative forcing for MIROC5-iso (Figure 4a). A correlation coefficient of -0.76 is found, agreeing with Lockwood (2002) who reported negative correlations ranging from -0.63 to -0.93 between the records of total solar irradiance and measured cosmic ray fluxes. The 11-year solar cycles are visible in the modeled HTO production and in the tritium of precipitation from the CRAC_3H_solar simulation (blue curves in Figure 4b and 4c, respectively). Significant changes in cosmogenic tritium production changes occur not only in the stratosphere but also in the mid-to high-troposphere (Figure S3 in Supporting Information S1). As a result, solar cycle-related changes in the tritium of tropospheric water vapor are clearly visible (Figures S4b and c in Supporting Information S1), explaining the presence of the 11-year solar cycle in tritium in precipitation. Temporal variations of tritium in stratospheric water vapor linked to solar cycles are also present even if they are slightly smoothed (Figures S4d and e in Supporting Information S1). At the global scale (i.e., land and ocean), modeled annual mean tritium of precipitation varies between 2.15 and 2.7 TU (blue curve in Figure 4c). Without such solar forcing for tritium production, the modeled tritium in precipitation is rather constant at the interannual time scale (CRAC_3H_cte simulation, orange curve in Figure 4c). The modeled tritium content in precipitation at Vostok from the CRAC_3H_solar simulation is in reasonably good agreement with the average data from the three snow pits after bomb contribution removal (Figure 4d). The time lags of approximately 2 years for some tritium peaks are within the range of uncertainty of the Vostok snow pit timescale. For the seasonal signals, MIROC5-iso underestimates the amplitude of interannual changes at Vostok (30–70 TU against 20 to 110 TU for the modeled and observed variations, respectively).

Depending on the location, tritium in precipitation is not similarly influenced by changes in HTO production owing to solar activity variations. Figure 5 shows the correlation and the slope of the linear regression between 1-

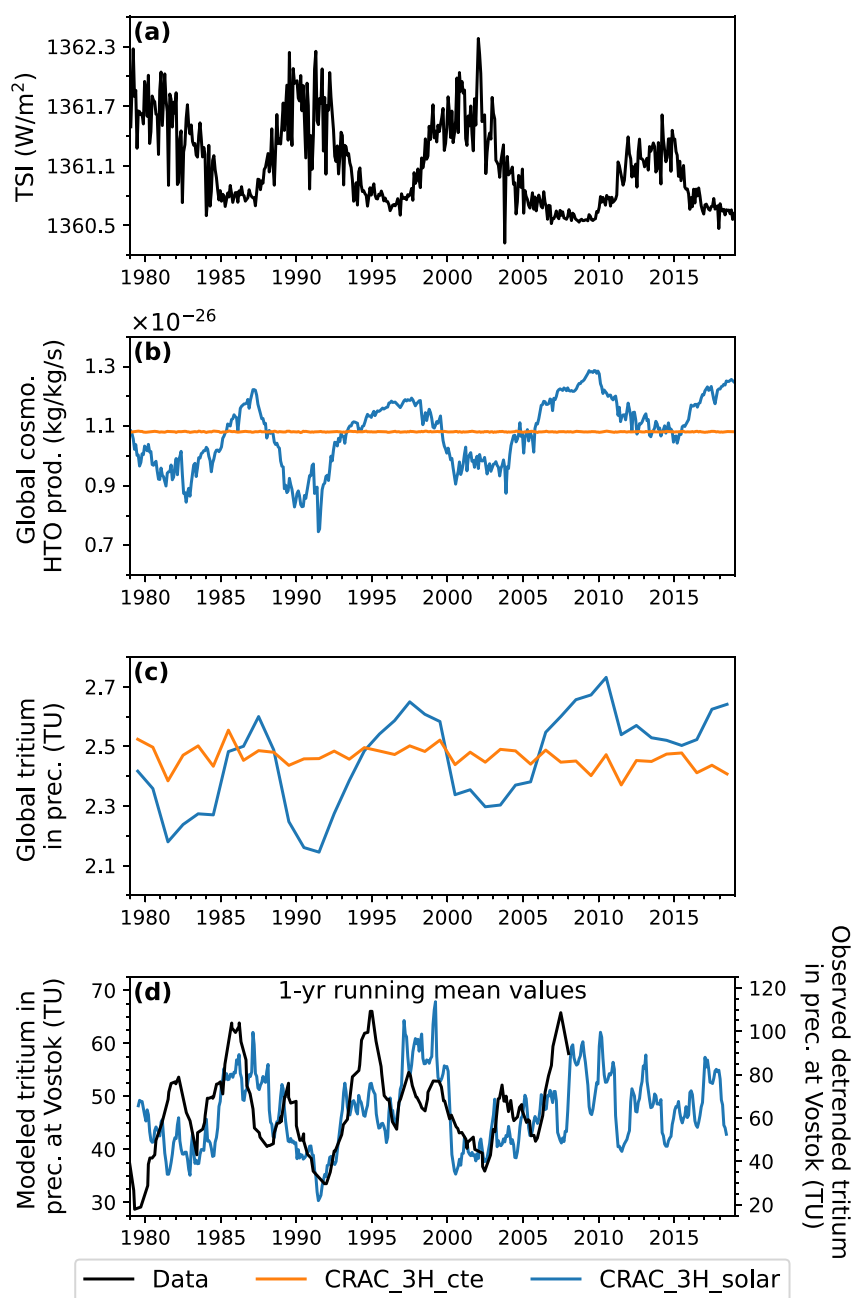


Figure 4. (a) CMIP6 total solar irradiance (TSI) used as radiative forcing for MIROC5-iso, (b) global mean modeled cosmogenic HTO production (expressed in kg of HTO per kg of air per second) depending on the tritium production rate function provided as input for MIROC5-iso, (c) global annual mean modeled tritium content of precipitation, and (d) comparison of 1-yr running mean values of modeled tritium in precipitation at Vostok from CRAC_3H_solar simulation with observations detrended from the bomb signal (Fourré et al., 2018). The black, orange, and blue curves correspond to the data (TSI and tritium at Vostok), and the modeled values from the simulations CRAC_3H_cte and CRAC_3H_solar, respectively.

year running mean tritium in precipitation and global HTO production from the CRAC_3H_solar simulation (Figure 4b) for each grid cell. Stronger correlations (i.e., >0.6) are found in the oceanic areas of the Southern Hemisphere, Atlantic Ocean, much of Antarctica, Europe, and Asia above 30° N (Figure 5a). Weaker modeled correlations in northeastern Greenland, tropical Pacific Ocean, and southern Asia could be due to the strong influence of moisture transport on the distribution of tritium in precipitation. Excessively dry conditions in far eastern Antarctica or parts of Africa could also partly explain the lower correlation between tritium content in

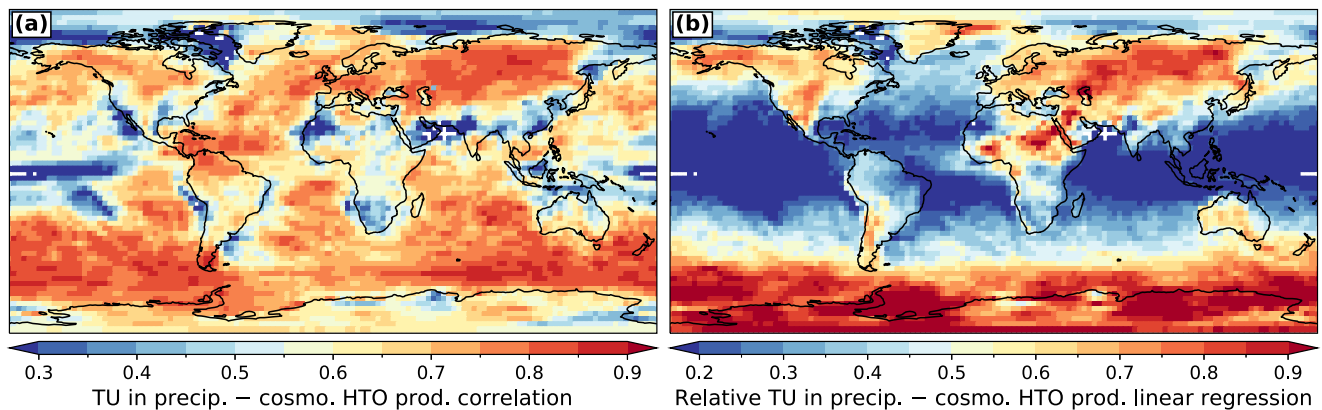


Figure 5. Correlation coefficients r (a) and slopes (b) of the linear regressions between 1-yr running mean tritium in precipitation and global HTO production from CRAC_3H_solar simulation for the period of 1979–2018. Only values that are significant at least at the 95% level are shown (i.e., p -value < 0.05).

precipitation and global HTO production (i.e., no record of production changes if there is no precipitation). The spatial distribution of linear regression coefficients between tritium in precipitation and HTO production (expressed relatively to the annual mean values of tritium in precipitation in each grid cell, Figure 5b) exhibits an ocean-land contrast in the Northern Hemisphere. Weaker values are simulated in low-to-mid ocean latitudes, while high values are located south of 50° S and in Northern Hemisphere land areas. In other words, the relatively strong correlation between tritium content in precipitation and tritium production rates in low-to mid-latitude ocean areas does not lead to significant changes in temporal tritium level variations.

4. Discussion: Solar Activity and Internal Climate Variability Influence on Tritium in Polar Precipitation

The link between tritium in precipitation and solar activity variations is not the same everywhere. For example, MIROC5-iso shows a clear contrast between the southern and northern polar regions. After tritium enters the hydrological cycle in the form of HTO directly after its production, tritium levels in precipitation are influenced by internal climate variability. For example, Fourré et al. (2018) suggested the influence of the Southern Annular Mode (SAM) on the tritium signal measured in the snow pits at Vostok. However, their analyses were limited by the fact that the tritium in precipitation modeled in LMDZ-iso did not depend on solar activity variations. Owing to the incorporation of the dependence of tritium production on past solar activity variations in MIROC5-iso, in this section, we investigate how internal climate variability modes can enhance or dampen the production component (i.e., related to solar activity changes) recorded in tritium of precipitation.

4.1. Effects of Southern Annular Mode on Tritium Levels in Antarctic Precipitation

The SAM defines how the southern westerly winds around the Antarctic continent contract or expand. In this study, we used the Marshall SAM index (Marshall, 2003) that is calculated as the difference in sea-level pressure between the latitudes of 40° S and 65° S (Figure 6b). During the positive phase of SAM (SAM+), the southern westerly winds contract, strengthening the circumpolar vortex and cooling most of Antarctica, except for the peninsula where warming occurs. This positive phase makes the East Antarctic plateau more isolated from oceanic moisture sources. For these reasons, variations in tritium in precipitation are positively correlated with changes in SAM in almost all of Antarctica, especially in the East Antarctic plateau (Figure 6c). In contrast, variations in the $\delta^{18}\text{O}$ of precipitation ($\delta^{18}\text{O}_p$) are inversely correlated with SAM changes because of the stronger cooling in the Antarctic inland during the SAM + phases (Figure 6d). For example, correlation values r of 0.28 and -0.20 are simulated for tritium in precipitation (CRAC_3H_solar simulation) and $\delta^{18}\text{O}_p$ at Vostok with SAM, respectively. We find a similar correlation between SAM changes and tritium in precipitation from the CRAC_3H_cte simulation ($r = 0.27$).

Tritium in precipitation signals at Vostok from the CRAC_3H_cte and CRAC_3H_solar simulations reveal common rapid interannual variations (i.e., two to 4 years, see orange and blue curves in Figure 6a, respectively) that may be linked to changes in the SAM (Figure 6b), similar to the local minimum in 1991 or the local maxima

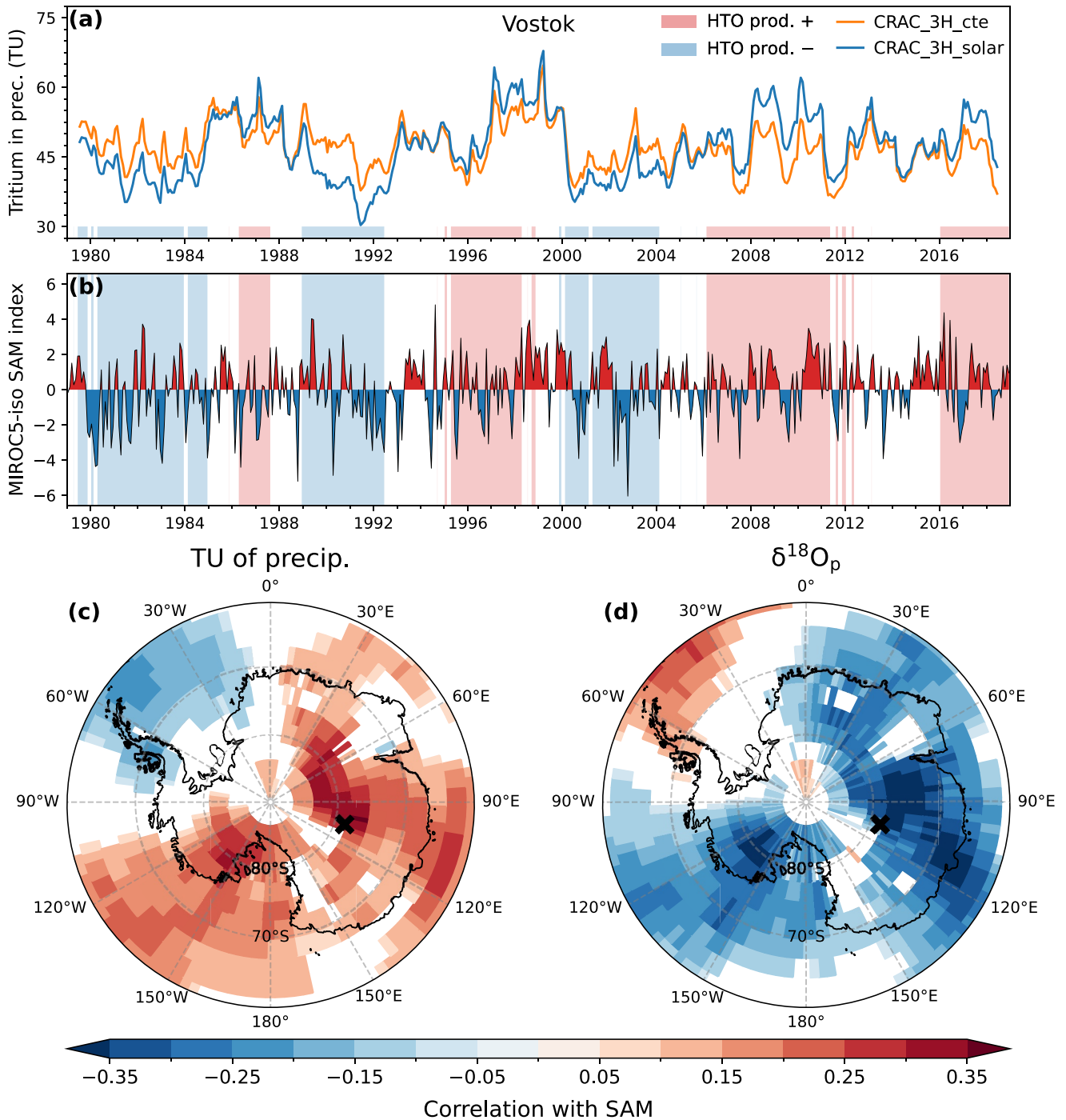


Figure 6. Impact of SAM on tritium in precipitation in Antarctica. (a) One-yr running mean tritium in precipitation at Vostok according to CRAC_3H_cte and CRAC_3H_solar simulations (orange and blue curves, respectively). (b) SAM index modeled by MIROC5-iso. For (a) and (b) plots, blue and red background colors correspond to periods with high and low production of natural HTO (defined as normalized global HTO production higher than 0.5 and lower than -0.5 , respectively). (c) Correlation coefficients of the linear regressions between monthly anomalies in tritium of precipitation from CRAC_3H_solar simulation and MIROC5-iso SAM index. (d) Same as (c) but for monthly anomalies in $\delta^{18}O_p$. Only values that are significant at least at the 95% level are shown (i.e., p -value < 0.05). The black cross indicates Vostok location. Monthly anomalies are calculated by subtracting from each monthly mean value the 1979–2018 mean value of the corresponding month (e.g., long-term January mean value subtracted from the January values).

in 1996–1999 and 2008–2011 periods. The decadal variations in the modeled tritium in precipitation from CRAC_3H_solar are due to variations in tritium production modulated by the 11-year solar cycles (blue curve in Figure 6a), as shown by the difference in tritium levels between the CRAC_3H_solar and CRAC_3H_cte

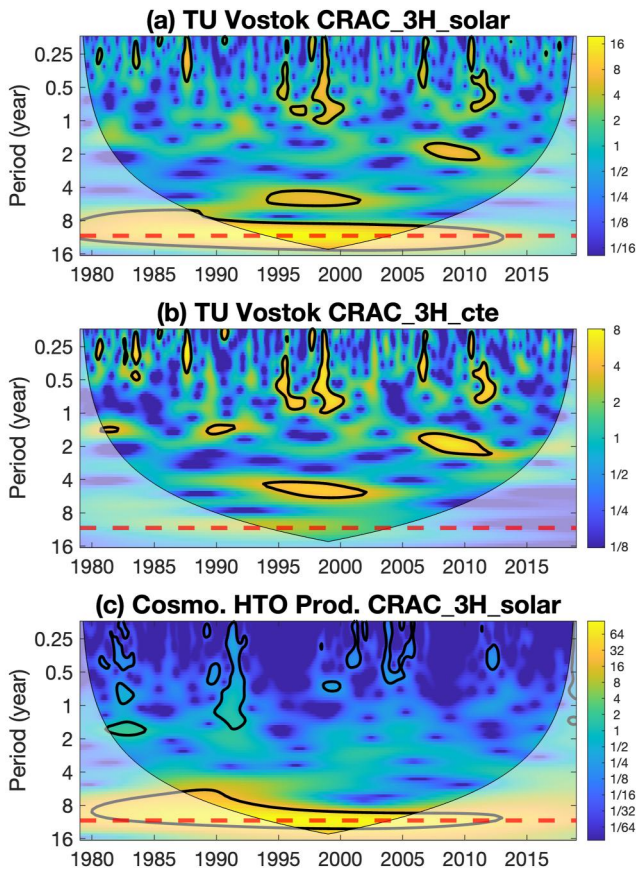


Figure 7. Wavelet analyses of monthly anomalies of modeled tritium in precipitation at Vostok from CRAC_3H_solar (a) and CRAC_3H_cte (b) simulations, and global cosmogenic HTO production from CRAC_3H_solar simulation (c). The colorbars indicate the wavelet power spectrum, expressed in σ^2 (i.e., time series variance). The red dashed lines represent the 11-yr period. The 5% significance level against red noise is shown as thick black contour. The wavelet analyses were performed with the MATLAB package from Grinsted et al. (2004).

simulations (Figure S5b in Supporting Information S1). The SAM phases and changes in relative tritium production are concomitant on several occasions during the period of 1979–2018, easing lower-frequency change detections in tritium in precipitation at Vostok. SAM– phases and lower tritium production rates are found in the 1979–1984, 1990–1992, and 2001–2003 periods (blue background color and blue filled curves in Figure 6b), whereas SAM + phases and higher tritium production rates are found for the periods around the year 1998, 2008–2011, and 2016–2018 (red background color and red filled curves in Figure 6b). In comparison, the periods when changes in SAM and solar activity have opposite impacts on tritium in precipitation are not so many and do not last over time (e.g., years 1989–1990 and 2001–2002). Consequently, the 11-year period due to the influence of solar activity on cosmogenic tritium production (Figure 7c) is evident in the tritium in precipitation at Vostok station (Figure 7a). As expected, the 11-year cycle is not present in the Vostok tritium time series modeled from the CRAC_3H_cte simulation (orange curve in Figures 6a and Figure 7b), confirming its cosmogenic origin.

4.2. North Atlantic Oscillation (NAO) Effect on Tritium Levels in Arctic Precipitation

The NAO is a large-scale atmospheric pressure see-saw occurring in the North Atlantic region. The main features are an area of relatively high pressure centered on the Azores Islands and an area of low pressure centered on Iceland. A positive NAO index (NAO+) indicates a greater pressure difference between these two zones, resulting in a stronger Atlantic jet stream and reinforced storm track activity. As a result, Greenland tends to be colder, with drier and wetter conditions in the western and eastern regions, respectively. In contrast, a negative NAO index (NAO–) indicates a weaker than usual pressure difference, with a latitudinal shift in the moisture source of Greenland precipitation towards the south, where warmer conditions occur. In our study, the NAO index (Figure 8c) is defined as the principal component time series of the leading empirical orthogonal function of the sea level pressure anomalies over the Atlantic sector (20°–80° N, 90° W–40° E) (Hurrell & Deser, 2009). An east-west contrast for the correlation of both tritium in precipitation and $\delta^{18}O_p$ with the NAO is modeled using MIROC5-iso (Figure 8d and 8e). Tritium in precipitation is positively correlated with NAO changes in western Greenland (drier in NAO+ phase), and negatively correlated with NAO in East Greenland (wetter in NAO+ phase). In contrast, $\delta^{18}O_p$ is inversely correlated with the NAO index in West Greenland because of changes in the location and temperature of source moisture of precipitation (Sodemann et al., 2008). The positive correlation between $\delta^{18}O_p$ and NAO in East Greenland is due to increased precipitation coming from the south coast during the NAO+ phase.

To investigate the east-west contrast response of tritium in precipitation to the NAO and its influence on the recording of solar cycles, we selected two Greenland stations: Camp Century in the west ([77.17° N; 61.13° W], $r = 0.27$) and Danmarkshavn in the east ([76.77° N; 18.67° W], $r = -0.26$). The difference between the tritium time series from the CRAC_3H_solar and CRAC_3H_cte simulations for these two sites (blue and orange curves in Figure 8a and 8b) shows well the presence of an 11-year solar cycle in tritium in local precipitation (Figures S5d and S5f in Supporting Information S1). However, the NAO has an important impact on the detection of 11-year solar cycles in Greenland precipitation tritium content. The NAO index values are more often of the opposite sign to variations in normalized tritium production (40.2% of the period of 1979–2018) than of the same sign (28.5% of the period). For example, strong NAO + phases and lower tritium production rates are concomitant for the periods of 1982–1984 and 1989–1992, and strong NAO– phases with higher tritium production rates are concomitant for the periods of 1995–1998 and 2008–2011 (Figure 8c). Therefore, tritium in precipitation in western Greenland is mainly influenced by two counteracting processes (e.g., the NAO + phase, which increases

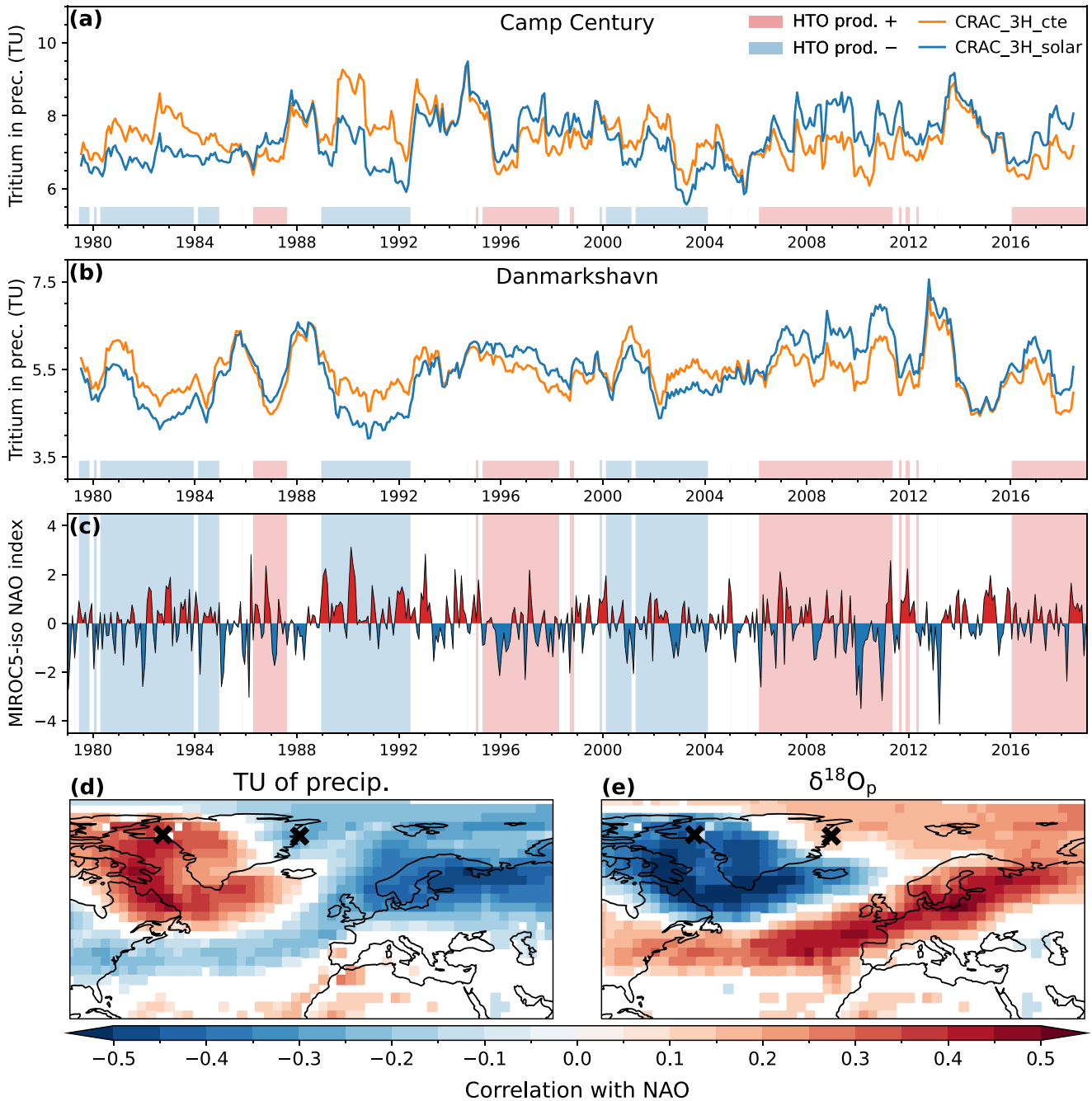


Figure 8. NAO impact on tritium in precipitation in the Arctic area. (a) One-yr running mean tritium in precipitation at Camp Century according to CRAC_3H_cte and CRAC_3H_solar simulations (orange and blue curves, respectively). (b) As (a) but for Danmarkshavn station. (c) NAO index modeled by MIROC5-iso. For (a), (b), and (c) plots, blue and red background colors correspond to periods with high and low production of natural HTO, respectively. (d) Correlation coefficients of the linear regressions between monthly anomalies in tritium of precipitation (CRAC_3H_solar simulation) and MIROC5-iso NAO index. (e) Same as (d) but for monthly anomalies in $\delta^{18}O_p$. Only values that are significant at least at the 95% level are shown (i.e., p-value < 0.05). The black crosses indicate the locations of Camp Century (western Greenland) and Danmarkshavn (eastern Greenland) stations.

tritium levels, and the lower tritium production, which decreases tritium levels in 1989–1992; Figure 8a), whereas the NAO influence on tritium in precipitation east of Greenland eases tritium production changes detection (Figure 8b). Thus, because of the NAO, an east-west contrast in the response of tritium in precipitation to solar cycles is modeled in MIROC5-iso, with a strong 11-year cycle at Danmarkshavn (Figure 9c) and the quasi-absence of such a cycle at Camp Century (Figure 9a). Again, the same tritium time series from the

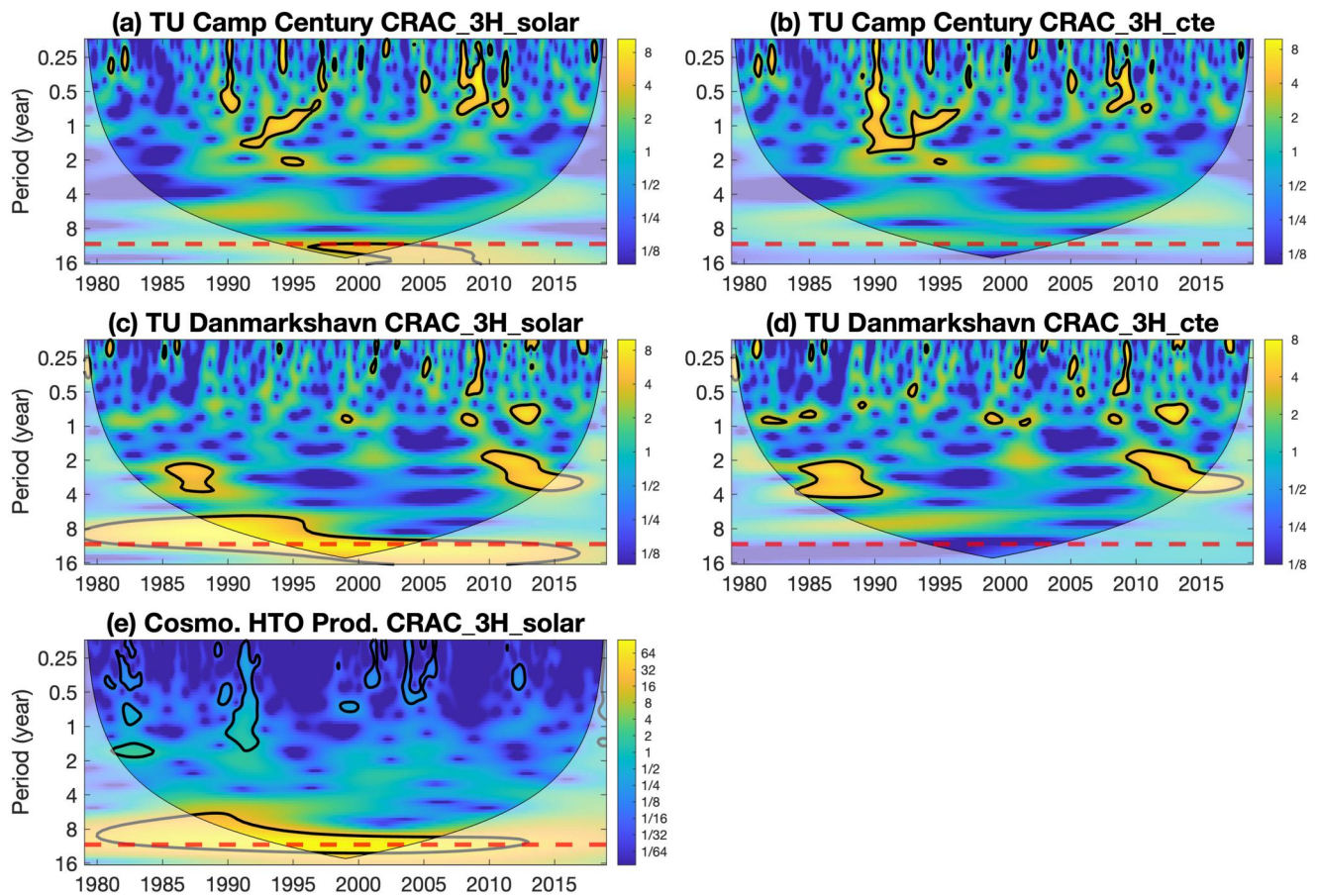


Figure 9. Wavelet analyses of monthly anomalies of modeled tritium in precipitation at Camp Century (from the simulations (a) CRAC_3H_solar and (b) CRAC_3H_cte) and Danmarkshavn (from the simulations (c) CRAC_3H_solar and (d) CRAC_3H_cte), and global cosmogenic HTO production from the CRAC_3H_solar simulation (e). The colorbars indicate the wavelet power spectrum, expressed in σ^2 (i.e., the time series variance). The red dashed lines represent the 11-yr period. The 5% significance level against red noise is shown as thick black contour. The wavelet analyses were performed with the MATLAB package from Grinsted et al. (2004).

CRAC_3H_cte simulation (orange curves in Figure 8a and 8b) do not show this 11-year solar cycle (Figure 9b and 9d). To our knowledge, there are no tritium observations in Greenland with sufficient temporal resolution over the post-bomb period (IAEA, 2023) or measurements with an instrument capable of detecting pre-bomb tritium levels in water samples (Qiao et al. (2021) were unable to measure tritium content below approximately 33 TU, which is not low enough), to confirm or refute our findings.

5. Conclusions and Perspectives

Natural tritium of water was implemented in the AGCM MIROC5-iso. In this study, the effects of solar activity on natural tritium production were considered for the first time. The effect of altitude on tritium content in water vapor, due to increased production and dry conditions as one ascends into the atmosphere, is well reproduced by MIROC5-iso, and agree well with previous observational and modeling studies. MIROC5-iso correctly reproduces the latitudinal and continental effects on tritium in precipitation, but with an underestimation compared to the observations. Seasonal variations in tritium in precipitation, linked to the stratosphere-troposphere mixing of water vapor, are very well modeled by MIROC5-iso in terms of timing despite the low amplitude of variations compared with observations. Possible reasons for this underestimation include a bias in the evaporation of tritiated water from the soil, or a too strong contribution from tritium-free ocean water. Finally, 11-year cycles linked to the influence of variations in solar activity on natural tritium production are well detected in our modeled tritium in precipitation. Adding this component to control tritium levels in water improves the agreement with contemporary tritium observations.

Because the tritium levels have nearly reached the pre-bomb levels, it is nowadays possible to investigate the influence of other factors on tritium in precipitation related to natural production variations and internal climate variability. Moreover, the use of state-of-the-art JRA-55 reanalyses to nudge MIROC5-iso simulations provided a good opportunity to reproduce weather conditions during our study period with higher accuracy. We focused our analyses on polar regions because tritium measurements in snow pits are very valuable for retrieving past variations of tritium in precipitation, in addition to other proxy tracers such as stable water isotopes. In addition, the Greenland and Antarctic regions differ in terms of the influence of moisture transport and stratosphere-troposphere transport on tritium in precipitation. The Greenland region is influenced by moisture transport from the Arctic and Atlantic oceans, whereas the Antarctic continent can be isolated by a strong polar vortex. Our modeled tritium in precipitation in East Antarctica is positively correlated with SAM variations, in agreement with Fourré et al. (2018). Colder conditions (especially in winter) and stronger polar vortex during SAM + phases increase tritium in precipitation in this area. As a result, SAM facilitates solar cycle-related production effect detection of tritium content in precipitation. The response of tritium in Greenland precipitation to the NAO is complex. We found an east-west contrast related to wet or dry conditions in the interior of Greenland and to the origin of the moisture source of precipitation. The positive correlation with the NAO in West Greenland hides the influence of tritium production variations, whereas the negative correlation of tritium in precipitation with the NAO in East Greenland reinforces this influence.

Tritium and $\delta^{18}O_p$ in precipitation generally respond oppositely to NAO and SAM (e.g., tritium in precipitation is correlated to SAM + at Vostok while $\delta^{18}O_p$ is anti-correlated to SAM+). While HTO and the stable isotopologues of water are both tracers of the water cycle, the impact of fractionation effects is lessened for the former because of its radioactive production and decay properties, resulting in substantially different concentrations in the different compartments of the water cycle (the stratosphere, soil, and ocean). For these reasons and as shown in this study, tritium and stable water isotopes can be considered complementary tracers, one being generally more a marker of the pathway between these reservoirs and the others efficiently tracing hydrological processes throughout the water cycle, such as evaporation and condensation. In this respect, the use of a fully coupled atmosphere-ocean model would make it possible to model tritium concentration in both the atmosphere and the ocean, the dynamics of exchanges within and between these water cycle reservoirs, and to dispense with the prescription of uncertain tritium boundary conditions at the sea surface.

Modeling tritium in an AGCM provides constraints on the transport and mixing of air masses between the stratosphere and troposphere. The use of the transient bomb peak forcing in climate simulations, which is large compared to changes in natural tritium production forcing, is one good way to evaluate the residence time of tritium in the stratosphere. For example, Cauquoin et al. (2016) found a decay time of approximately 4 years, which is lower than the estimation of 7.7 ± 2.0 years by Ehhalt et al. (2002). Moreover, considering the rather long residence time of tritiated water in the stratosphere, the mechanisms underlying the rapid response of tritium in precipitation to solar cycle-related production changes are still debated (Palcsu et al., 2018). According to our results in MIROC5-iso, we posit that significant changes in cosmogenic tritium production changes occur not only in the stratosphere but also in the mid-to high-troposphere. However, the temporal variations of tritium in stratospheric water vapor linked to solar cycles are present too, even if they are slightly smoothed. In a forthcoming study, we will simulate the tritium decay from bomb tests in MIROC5-iso, which has a more advanced advection scheme (Lin & Rood, 1996) than LMDZ-iso, using various state-of-the-art nudging reanalyses to more accurately assess the stratosphere-troposphere transport of tritiated water vapor.

Data Availability Statement

The GNIP data are available at <https://nucleus.iaea.org/wiser> (IAEA, 2023). Pre-bomb data are from Table S1 in Supporting Information S1 of Cauquoin et al. (2015). Contemporary tritium data were published by Terzer-Wassmuth et al. (2022a) and are openly available at <https://nucleus.iaea.org/sites/ihn/Pages/RCWIP.aspx> (Terzer-Wassmuth et al., 2022b). Tritium production rates from the CRAC:3H model are available in the supporting information of Poluianov et al. (2020) and the solar modulation potential from Usoskin et al. (2017) is freely accessible at <https://cosmicrays oulu.fi/phi/phi.html> (Usoskin, 2022). The code for the isotopic version MIROC5-iso, including the tritium branch, is available upon request from the private GitHub repository (<https://github.com/yoshimura-laboratory/MIROC5-iso>, Okazaki and Yoshimura (2019)). The MIROC5-iso outputs used

in this study and the monthly mean precipitation and tritium content outputs for the three simulations are available in the Zenodo database (<https://doi.org/10.5281/zenodo.10223858>, Cauquoin et al. (2023)).

Acknowledgments

We thank Jürgen Sültenfuß and two anonymous reviewers for their useful suggestions and comments that helped to substantially improve this article. The first author was supported by the Japan Society for the Promotion of Science (JSPS) KAKENHI Grant 22K20379. This study was also supported by JSPS Grants 21H05002 and 22H04938, MEXT program SENTAN (Grant JPMXD0722680395), ERCA S-20 (Grant JPMEEF21S12020), Arctic Challenge for Sustainability project phase 2 (ARCS2, JPMXD1420318865), and JST Grants JPMJSC22E4 and JPMJMI2116. We thank Stepan Poluianov (University of Oulu, Finland) for providing the natural tritium production rates from the CRAC:3H model. We also thank Stefan Terzer-Wassmuth for directly sending us the compilation of contemporary tritium data. We thank the Japan Meteorological Agency for the JRA-55 dataset, and the International Atomic Energy Agency for the compilation of isotope dataset GNIP.

References

Alken, P., Thébault, E., Beggan, C. D., Amit, H., Aubert, J., Baerenzung, J., et al. (2021). International geomagnetic reference field: The thirteenth generation. *Earth Planets and Space*, 73, 49. <https://doi.org/10.1186/s40623-020-01288-x>

Castagnoli, G., & Lal, D. (1980). Solar modulation effects in terrestrial production of carbon-14. *Radiocarbon*, 22(2), 133–158.

Cauquoin, A., Fourré, É., Landais, A., Okazaki, A., & Yoshimura, K. (2023). Cosmogenic tritium data modeled by MIROC5-iso [Dataset]. <https://doi.org/10.5281/zenodo.10223858>. Zenodo

Cauquoin, A., Jean-Baptiste, P., Risi, C., Fourré, É., & Landais, A. (2016). Modeling the global bomb tritium transient signal with the AGCM LMDZ-iso: A method to evaluate aspects of the hydrological cycle. *Journal of Geophysical Research: Atmospheres*, 121(21), 12612–12629. <https://doi.org/10.1002/2016JD025484>

Cauquoin, A., Jean-Baptiste, P., Risi, C., Fourré, É., Stenni, B., & Landais, A. (2015). The global distribution of natural tritium in precipitation simulated with an Atmospheric General Circulation Model and comparison with observations. *Earth and Planetary Science Letters*, 427, 160–170. <https://doi.org/10.1016/j.epsl.2015.06.043>

Cauquoin, A., & Werner, M. (2021). High-resolution nudged isotope modeling with ECHAM6-wiso: Impacts of updated model physics and ERA5 reanalysis data. *Journal of Advances in Modeling Earth Systems*, 13(11), e2021MS002532. <https://doi.org/10.1029/2021MS002532>

Chikira, M., & Sugiyama, M. (2010). A cumulus parameterization with state-dependent entrainment rate. Part I: Description and sensitivity to temperature and humidity profiles. *Journal of the Atmospheric Sciences*, 67(7), 2171–2193. <https://doi.org/10.1175/2010JAS3316.1>

Compo, G. P., Whitaker, J. S., Sardeshmukh, P. D., Matsui, N., Allan, R. J., Yin, X., et al. (2011). The twentieth Century reanalysis project. *Quarterly Journal of the Royal Meteorological Society*, 137, 1–28. <https://doi.org/10.1002/qj.776>

Craig, H., & Lal, D. (1961). The production rate of natural tritium. *Tellus*, 13(1), 85–105. <https://doi.org/10.1111/j.2153-3490.1961.tb00068.x>

Ehhalt, D. H., Rohrer, F., Schauffler, S., & Pollock, W. (2002). Tritiated water vapor in the stratosphere: Vertical profiles and residence time. *Journal of Geophysical Research*, 107, 4757. <https://doi.org/10.1029/2001JD001343>

Eyring, V., Bony, S., Meehl, G. A., Senior, C. A., Stevens, B., Stouffer, R. J., & Taylor, K. E. (2016). Overview of the coupled model Inter-comparison project phase 6 (CMIP6) experimental design and organization. *Geoscientific Model Development*, 9(5), 1937–1958. <https://doi.org/10.5194/gmd-9-1937-2016>

Fourré, É., Jean-Baptiste, P., Dapoigny, A., Baumier, D., Petit, J.-R., & Jouzel, J. (2006). Past and recent tritium levels in Arctic and Antarctic polar caps. *Earth and Planetary Science Letters*, 245, 56–64. <https://doi.org/10.1016/j.epsl.2006.03.003>

Fourré, É., Landais, A., Cauquoin, A., Jean-Baptiste, P., Lipenkov, V., & Petit, J.-R. (2018). Tritium records to trace stratospheric moisture inputs in Antarctica. *Journal of Geophysical Research: Atmospheres*, 123(6), 3009–3018. <https://doi.org/10.1002/2018JD028304>

Gat, J. R., Mook, W. G., & Meijer, H. J. (2001). Atmospheric water. In W. G. Mook (Ed.), *Environmental Isotopes in the hydrological cycle. Principles and applications, IHP-V technical documents in hydrology No. 39* (Vol. 2). UNESCO – IAEA. Retrieved from http://www-naweb.iaea.org/naweb/ihs_resources_publication_hydroCycle_en.html

Grinsted, A., Moore, J. C., & Jevrejeva, S. (2004). Application of the cross wavelet transform and wavelet coherence to geophysical time series. *Nonlinear Processes in Geophysics*, 11(5/6), 561–566. <https://doi.org/10.5194/npg-11-561-2004>

Harada, Y., Kamahori, H., Kobayashi, C., Endo, H., Kobayashi, S., Ota, Y., et al. (2016). The JRA-55 reanalysis: Representation of atmospheric circulation and climate variability. *Journal of the Meteorological Society of Japan*, 94(3), 269–302. <https://doi.org/10.2151/jmsj.2016-015>

Hurrell, J. W., & Deser, C. (2009). North atlantic climate variability: The role of the North atlantic oscillation. *Journal of Marine Systems*, 78(1), 28–41. <https://doi.org/10.1016/j.jmarsys.2008.11.026>

IAEA. (2023). International atomic energy agency/world meteorological organization. The GNIP Database. [Dataset]. Retrieved from <https://nucleus.iaea.org/wiser>. Global Network of isotopes in precipitation

Joussaume, S., Sadourny, R., & Jouzel, J. (1984). A general circulation model of water isotope cycles in the atmosphere. *Nature*, 311(5981), 24–29. <https://doi.org/10.1038/311024a0>

Jouzel, J., & Merlivat, L. (1984). Deuterium and oxygen 18 in precipitation: Modeling of the isotopic effects during snow formation. *Journal of Geophysical Research*, 89, 11749. <https://doi.org/10.1029/JD089iD07p11749>

Jouzel, J., Merlivat, L., Mazaudier, D., Pourchet, M., & Lorius, C. (1982). Natural tritium deposition over Antarctica and estimation of the mean global production rate. *Geophysical Research Letters*, 9, 1191–1194. <https://doi.org/10.1029/GL009i010p01191>

Jouzel, J., Merlivat, L., Pourchet, M., & Lorius, C. (1979). A continuous record of artificial tritium fallout at the South Pole (1954–1978). *Earth and Planetary Science Letters*, 45, 188–200. [https://doi.org/10.1016/0012-821X\(79\)90120-1](https://doi.org/10.1016/0012-821X(79)90120-1)

Jouzel, J., Russell, G. L., Suozzo, R. J., Koster, D., White, J. W. C., & Broecker, W. S. (1987). Simulations of the HDO and $\{H\}_2^18$ atmospheric cycles using the NASA GISS general circulation model: The seasonal cycle for present-day conditions. *Journal of Geophysical Research*, 92(D12), 14739–14760. <https://doi.org/10.1029/JD092iD12p14739>

Juhlke, T. R., Sültenfuß, J., Trachte, K., Huneau, F., Garel, E., Santoni, S., et al. (2020). Tritium as a hydrological tracer in Mediterranean precipitation events. *Atmospheric Chemistry and Physics*, 20(6), 3555–3568. <https://doi.org/10.5194/acp-20-3555-2020>

Kobayashi, S., Ota, Y., Harada, Y., Ebata, A., Moriya, M., Onoda, H., et al. (2015). The JRA-55 reanalysis: General specifications and basic characteristics. *Journal of the Meteorological Society of Japan*, 93(1), 5–48. <https://doi.org/10.2151/jmsj.2015-001>

Koster, R. D., Broecker, W. S., Jouzel, J., Suozzo, R. J., Russell, G. L., Rind, D., & White, J. W. C. (1989). The global geochemistry of bomb-produced tritium: General circulation model compared to available observations and traditional interpretations. *Journal of Geophysical Research*, 94, 18305–18326. <https://doi.org/10.1029/JD094iD15p18305>

Lal, D., & Peters, B. (1967). *Cosmic ray produced radioactivity on the Earth*. In K. Sittler (Ed.), *Kosmische strahlung II/cosmic rays II* (Vols. 46/2, pp. 551–612). Springer-Verlag. https://doi.org/10.1007/978-3-642-46079-1_7

Lee, J.-E., Fung, I., Depaolo, D. J., & Henning, C. C. (2007). Analysis of the global distribution of water isotopes using the NCAR atmospheric general circulation model. *Journal of Geophysical Research*, 112(D16), 16306. <https://doi.org/10.1029/2006JD007657>

Lin, S.-J., & Rood, R. B. (1996). Multidimensional flux-form semi-Lagrangian transport schemes. *Monthly Weather Review*, 124(9), 2046–2070. [https://doi.org/10.1175/1520-0493\(1996\)124<2046:MFFSLT>2.0.CO;2](https://doi.org/10.1175/1520-0493(1996)124<2046:MFFSLT>2.0.CO;2)

Lockwood, M. (2002). An evaluation of the correlation between open solar flux and total solar irradiance. *Astronomy and Astrophysics*, 382(2), 678–687. <https://doi.org/10.1051/0004-6361:20011666>

Lucas, L. L., & Unterwiesing, M. P. (2000). Comprehensive review and critical evaluation of the half-life of tritium. *Journal of Research of the National Institute of Standards and Technology*, 105(4), 541–549. <https://doi.org/10.6028/jres.105.043>

- Marshall, G. J. (2003). Trends in the southern annular mode from observations and reanalyses. *Journal of Climate*, *16*(24), 4134–4143. [https://doi.org/10.1175/1520-0442\(2003\)016<4134:TITSAM>2.0.CO2](https://doi.org/10.1175/1520-0442(2003)016<4134:TITSAM>2.0.CO2)
- Masarik, J., & Beer, J. (2009). An updated simulation of particle fluxes and cosmogenic nuclide production in the Earth's atmosphere. *Journal of Geophysical Research*, *114*, D11103. <https://doi.org/10.1029/2008JD010557>
- McFarlane, N. A. (1987). The effect of orographically excited gravity wave drag on the general circulation of the lower stratosphere and troposphere. *Journal of the Atmospheric Sciences*, *44*(14), 1775–1800. [https://doi.org/10.1175/1520-0469\(1987\)044<1775:TEOOEG>2.0.CO2](https://doi.org/10.1175/1520-0469(1987)044<1775:TEOOEG>2.0.CO2)
- Merlivat, L. (1978). Molecular diffusivities of H_2^{16}SO , HD^{16}O , and H_2^{18}SO in gases. *The Journal of Chemical Physics*, *69*(6), 2864–2871. <https://doi.org/10.1063/1.436884>
- Merlivat, L., & Jouzel, J. (1979). Global climatic interpretation of the deuterium-oxygen 18 relationship for precipitation. *Journal of Geophysical Research*, *84*(C8), 5029–5033. <https://doi.org/10.1029/JC084iC08p05029>
- Michel, R. L. (1976). Tritium inventories of the world oceans and their implications. *Nature*, *263*, 103–106. <https://doi.org/10.1038/263103a0>
- Nitta, T., Yoshimura, K., Takata, K., O'ishi, R., Sueyoshi, T., Kanae, S., et al. (2014). Representing variability in subgrid snow cover and snow depth in a global land model: Offline validation. *Journal of Climate*, *27*(9), 3318–3330. <https://doi.org/10.1175/JCLI-D-13-00310.1>
- Noone, D., & Simmonds, I. (2002). Associations between $\delta^{18}\text{O}$ of water and climate parameters in a simulation of atmospheric circulation for 1979–95. *Journal of Climate*, *15*(22), 3150–3169. [https://doi.org/10.1175/1520-0442\(2002\)015<3150:ABOWA>2.0.CO2](https://doi.org/10.1175/1520-0442(2002)015<3150:ABOWA>2.0.CO2)
- Nusbaumer, J., Wong, T. E., Bardeen, C., & Noone, D. (2017). Evaluating hydrological processes in the Community Atmosphere Model Version 5 (CAM5) using stable isotope ratios of water. *Journal of Advances in Modeling Earth Systems*, *9*(2), 949–977. <https://doi.org/10.1002/2016ms000839>
- Okazaki, A., & Yoshimura, K. (2019). Global evaluation of proxy system models for stable water isotopes with realistic atmospheric forcing. *Journal of Geophysical Research: Atmospheres*, *124*(16), 8972–8993. <https://doi.org/10.1029/2018JD029463>
- Palcsu, L., Morgenstern, U., Sültenfuss, J., Koltai, G., László, E., Temovski, M., et al. (2018). Modulation of cosmogenic tritium in meteoric precipitation by the 11-year cycle of solar magnetic field activity. *Scientific Reports*, *8*(1), 12813. <https://doi.org/10.1038/s41598-018-31208-9>
- Poluianov, S. V., Kovaltsov, G. A., & Usoskin, I. G. (2020). A new full 3-D model of cosmogenic tritium ^3H production in the atmosphere (CRAC:3H). *Journal of Geophysical Research: Atmospheres*, *125*(18), e2020JD033147. <https://doi.org/10.1029/2020JD033147>
- Qiao, J., Colgan, W., Jakobs, G., & Nielsen, S. (2021). High-resolution tritium profile in an ice core from Camp Century, Greenland. *Environmental Science and Technology*, *55*(20), 13638–13645. <https://doi.org/10.1021/acs.est.1c01975>
- Risi, C., Bony, S., Vimeux, F., & Jouzel, J. (2010). Water-stable isotopes in the LMDZ4 general circulation model: Model evaluation for present-day and past climates and applications to climatic interpretations of tropical isotopic records. *Journal of Geophysical Research*, *115*(D14), 12118. <https://doi.org/10.1029/2009JD013255>
- Roscoe, H. K. (2004). Possible descent across the “tropopause” in antarctic winter. *Advances in Space Research*, *33*(7), 1048–1052. [https://doi.org/10.1016/S0273-1177\(03\)00587-8](https://doi.org/10.1016/S0273-1177(03)00587-8)
- Sodemann, H., Masson-Delmotte, V., Schwierz, C., Vinther, B. M., & Wernli, H. (2008). Interannual variability of Greenland winter precipitation sources: 2. Effects of North Atlantic oscillation variability on stable isotopes in precipitation. *Journal of Geophysical Research*, *113*, D12111. <https://doi.org/10.1029/2007JD009416>
- Stewart, M. K. (1975). Stable isotope fractionation due to evaporation and isotopic exchange of falling waterdrops: Applications to atmospheric processes and evaporation of lakes. *Journal of Geophysical Research*, *80*(9), 1133–1146. <https://doi.org/10.1029/JC080i009p01133>
- Takata, K., Emori, S., & Watanabe, T. (2003). Development of the minimal advanced treatments of surface interaction and runoff. *Global and Planetary Change*, *38*(1–2), 209–222. [https://doi.org/10.1016/S0921-8181\(03\)00030-4](https://doi.org/10.1016/S0921-8181(03)00030-4)
- Terzer-Wassmuth, S., Araguás-Araguás, L. J., Copia, L., & Wassenaar, L. I. (2022a). High spatial resolution prediction of tritium (^3H) in contemporary global precipitation. *Scientific Reports*, *12*(1), 10271. <https://doi.org/10.1038/s41598-022-14227-5>
- Terzer-Wassmuth, S., Araguás-Araguás, L. J., Copia, L., & Wassenaar, L. I. (2022b). Regionalized cluster-based water isotope prediction. [Dataset]. Retrieved from <https://nucleus.iaea.org/sites/ihp/Pages/RWCWP.aspx>. Version 2 (RCWIP2) and 3H isoscape
- Thébault, E., Finlay, C. C., Beggan, C. D., Alken, P., Aubert, J., Barrois, O., et al. (2015). International geomagnetic reference field: The 12th generation. *Earth Planets and Space*, *67*, 79. <https://doi.org/10.1186/s40623-015-0228-9>
- UNSCEAR. (2000). In annex C (tech. Rep.). United nations. United nation scientific committee on the effects of atomic radiations. Retrieved from https://www.unscear.org/unscear/en/publications/2000_1.html. Sources and effects of ionizing radiation: Reports to the general assembly with scientific annexes volume 1
- Usoskin, I. G. (2022). Cosmic ray modulation potential (Φ) reconstructed from ground-based neutron-monitor data. [Dataset]. Retrieved from <https://cosmicrays oulu.fi/phi/phi.html>
- Usoskin, I. G., Gil, A., Kovaltsov, G. A., Mishev, A. L., & Mikhailov, V. V. (2017). Heliospheric modulation of cosmic rays during the neutron monitor era: Calibration using PAMELA data for 2006–2010. *Journal of Geophysical Research: Space Physics*, *122*(4), 3875–3887. <https://doi.org/10.1002/2016JA023819>
- Vos, E. E., & Potgieter, M. S. (2015). New modeling of galactic proton modulation during the minimum of solar cycle 23/24. *The Astrophysical Journal*, *815*(2), 119. <https://doi.org/10.1088/0004-637X/815/2/119>
- Watanabe, M., Emori, S., Satoh, M., & Miura, H. (2009). A PDF-based hybrid prognostic cloud scheme for general circulation models. *Climate Dynamics*, *33*(6), 795–816. <https://doi.org/10.1007/s00382-008-0489-0>
- Watanabe, M., Suzuki, T., O'ishi, R., Komuro, Y., Watanabe, S., Emori, S., et al. (2010). Improved climate simulation by MIROC5: Mean states, variability, and climate sensitivity. *Journal of Climate*, *23*(23), 6312–6335. <https://doi.org/10.1175/2010JCLI3679.1>
- Werner, M., Langebroek, P. M., Carlsen, T., Herold, M., & Lohmann, G. (2011). Stable water isotopes in the ECHAM5 general circulation model: Toward high-resolution isotope modeling on a global scale. *Journal of Geophysical Research*, *116*(D15), 15109. <https://doi.org/10.1029/2011JD015681>
- Wilson, D. R., & Ballard, S. P. (1999). A microphysically based precipitation scheme for the UK meteorological office unified model. *Quarterly Journal of the Royal Meteorological Society*, *125*(557), 1607–1636. <https://doi.org/10.1002/qj.49712555707>
- Yoshimura, K., Kanamitsu, M., Noone, D., & Oki, T. (2008). Historical isotope simulation using Reanalysis atmospheric data. *Journal of Geophysical Research*, *113*(D19), 19108. <https://doi.org/10.1029/2008JD010074>
- Yoshimura, K., Miyazaki, S., Kanae, S., & Oki, T. (2006). Iso-MATSIRO, a land surface model that incorporates stable water isotopes. *Global and Planetary Change*, *51*(1–2), 90–107. <https://doi.org/10.1016/j.gloplacha.2005.12.007>